ACS APPLIED MATERIALS & INTERFACES

RESEARCH ARTICLE

www.acsami.org

Enzyme Biosensor Based on Plasma-Polymerized Film-Covered Carbon Nanotube Layer Grown Directly on A Flat Substrate

Hitoshi Muguruma,* Tatsuya Hoshino, and Yasunori Matsui

Department of Electronic Engineering, Shibaura Institute of Technology, 3-7-5 Toyosu, Koto-ku, Tokyo 135-8548, Japan

Supporting Information

ABSTRACT: We report a novel approach to fabrication of an amperometric biosensor with an enzyme, a plasma-polymerized film (PPF), and carbon nanotubes (CNTs). The CNTs were grown directly on an island-patterned Co/Ti/Cr layer on a glass substrate by microwave plasma enhanced chemical vapor deposition. The as-grown CNTs were subsequently treated by nitrogen plasma, which changed the surface from hydrophobic to hydrophilic in order to obtain an electrochemical contact between the CNTs and enzymes. A glucose oxidase (GOx) enzyme was then adsorbed onto the CNT surface and directly treated with acetonitrile plasma to overcoat the GOx layer with a PPF. This fabrication process provides a robust design of CNT-based enzyme biosensor, because of all processes are dry except the procedure for enzyme immobilization. The main novelty of the present methodology lies in the PPF and/or plasma processes. The optimized glucose biosensor revealed a high sensitivity of 38 μA mM^{-1} cm^{-2}, a broad linear dynamic range of 0.25−19 mM (correlation coefficient of 0.994), selectivity toward an interferent (ascorbic acid), and a fast response time of 7 s. The background current was much smaller in magnitude than the current due to 10 mM glucose response. The low limit of detection was 34 μM (S/N = 3). All results strongly suggest that a plasma-polymerized process can provide a new platform for CNT-based biosensor design.

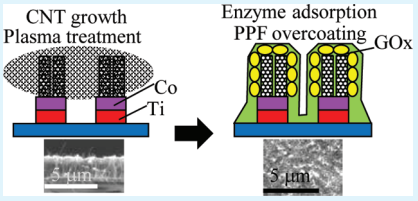

KEYWORDS: plasma-polymerized film, amperometric biosensor, glucose oxidase, carbon nanotube, direct grown on substrate, acetonitrile monomer

INTRODUCTION

Development of an amperometric biosensor based on biospecific enzyme reaction has become an active research area because biosensors play an important role in clinical diagnosis, such as precise monitoring of blood sugar level for diabetes.[1,2] A key factor in developing amperometric biosensors is the coupling of the biological component (enzyme) to the surface of the electrode as a transducer. This aspect of biosensor development is often referred to as interfacial design. In recent years, major developments have been made to increase biosensor performance by incorporating various nanostructured materials into the interfacial design. The nanomaterials employed include carbon nanotubes (CNTs),[3,4] carbon nanofiber,[4] graphene,[5] graphitic nanocages,[6] gold nanocoral,[7] metal (Au, Pt, Pd) nanoparticles,[8] zinc oxide nanofiber,[9,10] and zinc oxide nanotubes.[11] The main reason for the utilization of nanomaterials is that their inherently vast surface-to-volume ratios offer higher enzyme loading and a more effective contact between the deeply buried active sites of enzymes and the electrode, which could dramatically improve the sensor performance.

We have focused on CNTs, which are one of the most promising nanomaterials for biosensors. CNTs are the result of folding graphene layers into carbon cylinders, and consist of single or multiple hollow cylindrical graphene layers. CNTs display excellent electrical conductivity, excellent catalytic activity, high mechanical strength, and high chemical stability. In recent years, much research on amperometric enzyme biosensors that employ CNTs have been reported.[1−4,12−23] The typical structure of a CNT-based amperometric biosensor is a combination of biomolecules (e.g., enzymes) and powdered CNTs in the vicinity of an electrode. There are two requirements for desirable sensor performance; one is the hydrophobic surface of the CNTs must be changed to a hydrophilic surface in order to be combined with enzymes when used in the aqueous phase, and the other is an appropriate interface design between the CNTs and enzymes to obtain sufficient electron transfer from the reaction center of the enzyme to the electrode via the CNTs. One strategy to address these requirements includes the introduction of chemically active functional groups by treatment of CNTs with sulfuric or nitric acid, which then enables subsequent modification.[12−18] The subsequent modification involves the dispersion of CNTs within a polymer matrix such as Nafion,[14] a polyelectrolyte,[15] or other polymers.[16−19] However, those contain the cumbersome steps, such as washing to clean the CNTs. These methods also require that the enzymes and other biomolecules receive careful treatment in order to retain their tertiary structure. Therefore, our motivation is simplification of the fabrication processes.

On the other hand, there are problematic aspects of using "powdered" CNT materials: (i) poor reproducibility in terms of alignment and placement of powdered CNT with respect to the enzyme and electrode, and (ii) poor contact between the powder CNT and electrode, which results in poor electrical conductivity.

Received: March 18, 2011
Accepted: June 17, 2011
Published: June 17, 2011

A current approach is to use directly grown CNTs,[20−23] in which a monomer gas such as methane is used to grow CNTs on the metal surface as a catalyst using microwave plasma enhanced chemical vapor deposition. However, these methodologies still involve problems in that the as-grown CNTs must be subsequently modified by "wet" chemical processes, such as treatment with H_2SO_4,[20] NaOH,[21] and HNO_3,[22] and electrochemical deposition.[23] These reported strategies do not maintain the advantage of direct CNT growth. Therefore, a complete fabrication technique has yet to be devised.

We have reported a biosensor based on a plasma-polymerized thin film (PPF) and/or plasma modification.[24] PPFs were created in a glow discharge under a monomer vapor phase, which resulted in the direct deposition of a thin film on the substrate. Plasma modification with a nonpolymerized monomer gas provides a simple method for control of the surface properties. "Dry" plasma modification directly toward CNTs can change their hydrophobicity to hydrophilicity, while maintaining the CNT properties. Enzymes adsorbed onto the CNTs were subsequently overcoated by a plasma polymerization film. As a result, the working electrode exhibited excellent performance, due to suitable electrochemical contact between the reaction center of the enzyme and the CNT layer.[25] Therefore, PPFs are suitable for the interfacial design between an enzyme and an electrode. Furthermore, the advantage of this technique is to enhance the efficiency of the fabrication process, because the CNTs are directly grown on the flat electrode in a dry process. A continuously dry process can be provided throughout manufacturing, except during enzyme immobilization. CNTs were directly grown on a Co/Ti/Cr layered structure on a glass substrate by microwave plasma enhanced chemical vapor deposition of a methane/hydrogen mixture. In this article, we propose a novel and simple strategy for the interfacial design of a CNT-based amperometric biosensor.

EXPERIMENTAL DETAILS

Materials. Distilled water, potassium dihydrogenphosphate, disodium hydrogenphosphate, *D*-glucose, ethanol, hydrogen peroxide, ammonia, and acetonitrile were purchased from Kanto Chemical Inc., (Tokyo, Japan). Glucose oxidase (GOx) obtained from *Aspergillus niger* (EC 1.1.3.4, type VII−S, 181 600 units g^{-1}, Sigma, St. Louis, MO) was used as the enzyme. All reagents were used without further purification.

Fabrication Procedure. An amperometric biosensor based on CNTs, PPF, and GOx was fabricated with a unique sandwich-like structure; PPF/GOx/CNT/Co/Ti/Cr. The electrochemical device as a working electrode was fabricated using a dry-chemistry layer-by-layer process. A schematic representation of the fabrication procedure is shown in Figure 1. The device as a working electrode was formed onto a 0.15 mm thick quartz glass substrate. All the metal layers were sputter-deposited and patterned by a masking process. The glass slides used to make the thin film electrodes were boiled in a hydrogen peroxide/ammonia/water solution (approximately 1:1:8 by volume) for 1 h, and then rinsed with water and acetone. A 150 nm thick Cr thin film was first deposited using sputtering apparatus to promote adhesion between the subsequent Ti layer and the glass substrate. In order to make the spacing for CNT growth, a circle-punched shadow mask (200 μm diameter punched circle, 200 or 400 μm pitch) was placed onto the Cr surface. A 10 nm thick Ti layer and 10 nm thick Co layer were then sequentially formed. CNT growth was started from the Co layer by microwave enhanced chemical vapor deposition using the cobalt as a catalyst. A schematic diagram of the plasma apparatus is shown in Figure S1 in the Supporting Information. The substrate was placed downstream of the plasma. A metal mesh placed between the plasma generator and the substrate removes ionic species (cations and anions) in the plasma, so that the polymerization process occurs only in the presence of radical species. The substrate was heated to 650 °C in a mixture of methane and hydrogen using a 3 kW microwave power supply. The pressure was 267 Pa and the flow rates of methane and hydrogen were 20 and 80 cm^3 min^{-1}, respectively. The CNT growth rate was 75 nm min^{-1}. The surface of the as-grown CNTs was treated with nitrogen plasma under the following parameters: power, 100 W (optimized); flow rate, 15 mL min^{-1}; pressure, 3 Pa; exposure time, 60 s. The enzyme was then added by dropping an aliquot of GOx (10 mg mL^{-1}) in phosphate buffer (20 mM, pH 7.4) onto the modified CNT surface. The GOx concentration has been optimized by our previous work[26] in which the adsorption of GOx protein on the plasma modified surface follows the Langmuir isotherm. The adsorbed GOx on plasma modified surface formed as the densely two-dimensional packed array and did not as the multilayer adsorption. The threshold concentration for densely pack formation was around 0.1 mg/mL. The surface was washed with water 1 h after enzyme immobilization. Finally, the enzyme-adsorbed surface was overcoated with an acetonitrile-PPF. A plasma generator (VEP-1000, Ulvac Inc., Tokyo, Japan) was used to deposit a 13 nm thick acetonitrile-PPF at 150 W under a pressure of 0.6 Pa. The deposition rate was ca. 5 nm min^{-1}. The as-fabricated devices were stored in a refrigerator at 4 °C until use. In the time for measurement, it is picked out and put into the buffer solution. The dimension of the opening for the working electrode was 5.3 mm^2 (optimized sample, see the Figure S2 in the Supporting Information).

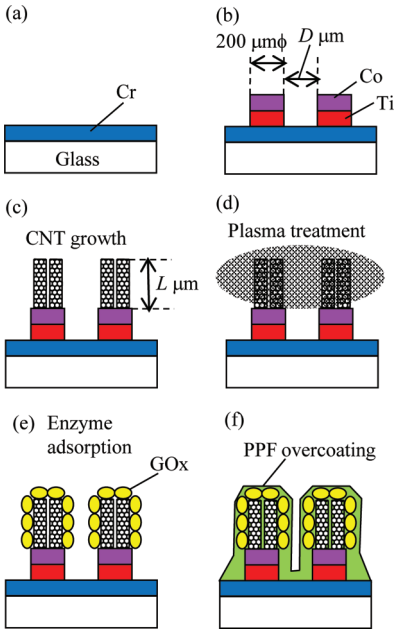

Figure 1. Schematic representation of the fabrication process for an amperometric biosensor based on CNTs and a PPF. (a) 150 nm thick Cr layer sputtered onto glass substrate through a metal mask. (b) 10 nm thick Co and Ti layers sputtered through a shadow mask. (c) CNTs directly grown on substrate. (d) Nitrogen or oxygen plasma treatment of the CNT layer. (e) Solution casting of the enzyme layer onto the CNT layer. (f) Immobilized GOx overcoated with a 13 nm thick acetonitrile PPF.

Measurements. Electrochemical measurements were performed with an electrochemical analyzer (ALS Instruments, 701A West Lafayette, IN) using a three-electrode configuration. A reference electrode (Ag/AgCl, RE-1C) and a counter electrode (platinum wire) were purchased from Bioanalytical Systems Inc. Electrical measurements

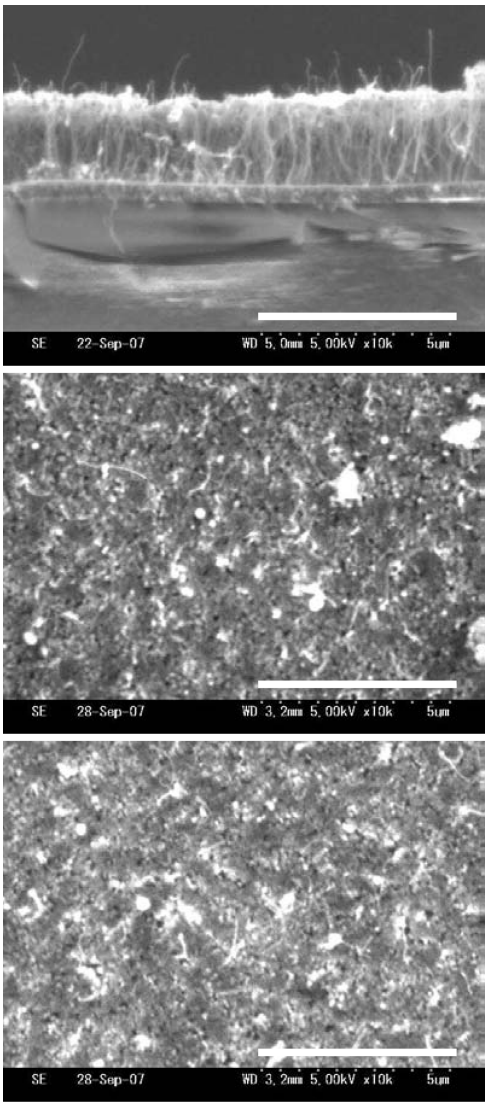

Figure 2. SEM images: (a) cross-sectional image of the CNT layer, (b) CNT layer surface, (c) CNT surface with immobilized enzyme and PPF. The scale bar corresponds to 5 μm.

were conducted in a 10 mL vessel at ambient temperature (22 °C) using a phosphate buffer (20 mM, pH 7.4) as the supporting electrolyte. To prepare samples at designated concentrations, stock glucose solutions of 25 or 250 mM were successively added. Electrochemical measurements were carried out at least four times. Scanning electron microscopy (SEM; Hitachi S-800) was performed at an operation voltage of 6 kV.

RESULTS AND DISCUSSION

Optimization of Fabrication Procedure. Figure 2a shows a cross sectional SEM image of the as-grown CNTs, which confirms that CNTs were grown almost perpendicular to the Co-coated substrate. The CNT surface can therefore provide a conductive pathway for electron transfer, unlike powder CNTs assembled by casting or spin-coating of a dispersed CNT solution. The diameter of the observed CNTs was estimated to be 70−80 nm from Figure 2a, which suggests that these are multiwalled CNTs. Figure 2b shows an SEM image of the CNT surface with no evidence of distinct CNT fibers, which indicates

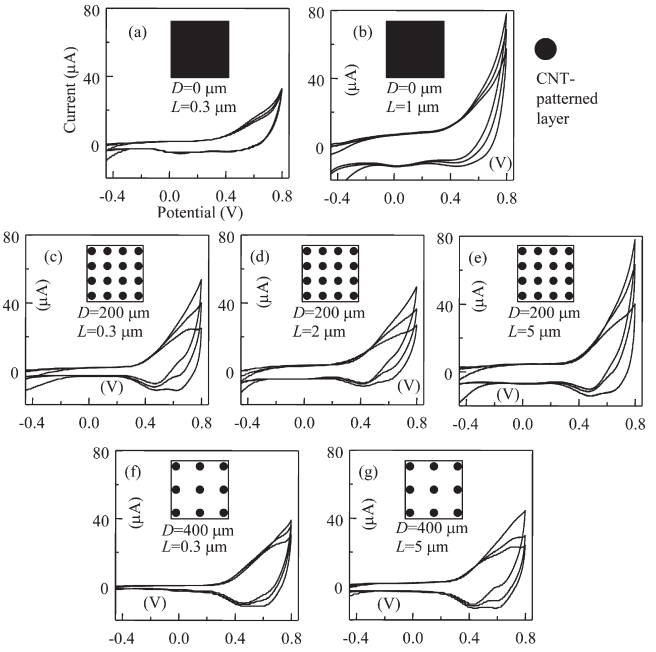

Figure 3. Cyclic voltammetry for the biosensor response in the absence and presence of glucose. The sweep rate was 50 mV s^{-1} and the glucose concentrations were 0, 17, and 48 mM. The electrolyte used was a pH 7.4, 20 mM phosphate buffer solution. The structure of the device was PPF/GOx/CNT/Co/Ti/Cr. Parameters are CNT length (L) perpendicular to the substrate and pitch (D) for the in-plane CNT pattern.

that the CNTs were grown straight and perpendicular to the substrate; closely packed bundles of multiwalled CNTs were obtained.

Figure 2c shows a SEM image of the surface of the fabricated device containing the immobilized enzyme. Compared to the as-grown CNT surface in Figure 2b, the surface of Figure 2c appears to be rougher and thicker, which indicates that the enzyme molecules adsorbed to CNT surface were successfully overcoated by a nanothin PPF. Although individual molecules cannot be observed in the SEM image, we speculate that the 13 nm thick PPF layer provides a coating to completely cover the adsorbed enzyme GOx, of which the height of the monolayer at the surface is 6−7 nm.[26] The hydrophilic acetonitrile PPF is easily deposited onto the hydrophilic protein (GOx) layer, as confirmed by the observation with atomic force microscopy.[27]

The configuration parameters of the CNT layer are critical in this experiment, because the formation of an interface structure between the enzyme molecules and CNT layer determines the performance of the biosensor. The two configuration parameters: one is the CNT length perpendicular to the substrate, L = 0.3, 1, 2, and 5 μm (Figure 1c), and the other is the spacing of CNT islands; 200 μm diameter CNT circles are placed with pitches of D = 0, 200, and 400 μm, where D = 0 represents a CNT layer formed over the entire substrate surface (Figures 1a and 1b). These parameters concern the amount of enzyme loading, the contact area between enzymes and CNTs, and both the conductivity and catalytic activity of the CNT layer, which strongly affect the sensor performance.

Cyclic voltammetry (CV) is a useful tool for fundamental evaluation of the modified electrode. The results of CV for the biosensor response to glucose are shown in Figure 3. A working electrode that was completely overcoated by CNTs (D = 0)

showed a poor current in response to glucose addition (Figures 3a and 3b). In contrast, the electrode with an area partially covered in CNTs (D = 200 and 400) exhibited an improved response current, as shown in Figures 3c-g. This improved response is probably due to an increase in the contact area between the CNTs and the reaction center of enzymes. As a result, hydrogen peroxide caused by enzymatic reaction is efficiently catalyzed, and subsequently transported toward the Cr electrode as an electron collector. In a word, increasing the contact area between the CNTs and GOx increased the mass transport (diffusion) of hydrogen oxide from the reaction center of GOx to CNT layer. The signal for D = 400 (Figure 3e,f) is smaller than that for D = 200 (Figure 3c−e), which indicates that the D = 400 pitch is too wide to obtain a sufficient signal because of a lack of CNTs.

This result demonstrates the effectiveness of CNT island formation, which is also shown by the amperometric measurement at fixed potential in which the response time of the working electrode with no spacing (D = 0) in Figure 3b (40 s, see Figure S3a in the Supporting Information) was much slower than that with spacing (D = 200) in Figure 3c (7 s, see Figure S3b in the Supporting Information). Therefore, the formation CNT-patterning by direct growth is mandatory for suitable sensor performance. Similar strategies taken by other researchers have been utilization of porous anodic alumina[23] and passivation by an epoxy resin layer.[21]

With respect to the CNT length (L) in Figures 3c−e (D = 200), increase of the CNT length (L) caused a higher background current. The higher background current showed the worse linearity for the calibration. Additionally, it brings the failed signal such as unstable baseline and noise. The fact is distinct in the time-current plot at fixed potential shown in Figure S3c in the Supporting Information (Figure 3e). Therefore, it was concluded that the optimum CNT configuration parameters are L = 0.3 μm and D = 200 μm (Figure 3c).

Mechanisms can be considered for the large current response based on the catalytic activity of the CNTs[3] toward hydrogen peroxide generated by the enzymatic reaction. GOx specifically catalyzes the oxidation of glucose as follows

$$\beta\text{-D-glucose} + O_2 \xrightarrow{\text{GOx}} \text{D-gluconic acid} + H_2O_2 \qquad (1)$$

and the CNT catalyzes the reaction of hydrogen peroxide as follows

$$H_2O_2 \rightarrow 2H^+ + O_2 + 2e^- \qquad (2)$$

The increase in current at greater than 0.6 V in the CV profiles shown in Figure 3 corresponds to reaction 2. The smaller response in nitrogen-saturated (oxygen depletion) glucose solution than that in air-saturated glucose solution supports the above mechanism.

We stress the advantage of nitrogen plasma treatment. Nitrogen plasma treatment of the CNT surface for only 1 min can improve the biocompatibility of CNTs without degradation of the CNT properties. In contrast, a wet chemical process consumes requires longer processing times (long reaction time and washing). The effectiveness of nitrogen plasma treatment is due to the introduction of amino groups to the side wall surface of the CNTs,[25,28] which results in the hydrophobic surface of the CNTs being changed to a stable hydrophilic environment that facilitates contact with GOx. Negatively charged GOx (pI = 4.2) can then be densely loaded onto the positively charged CNT surfaces.[26] Moreover, a dry plasma process is continuous to a dry direct CNT growth process, unlike wet-chemical-based processes used with powdered CNTs.

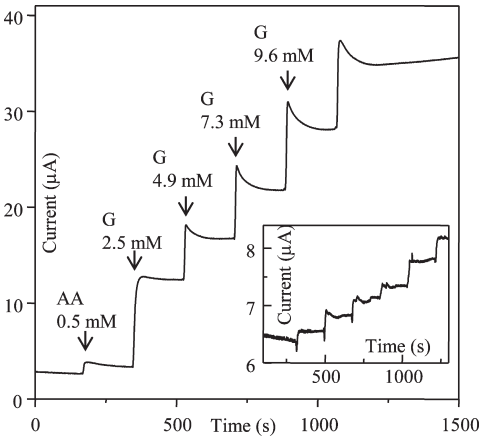

Figure 4. Time−current response for sequential glucose (G) addition at concentrations of 0, 2.5, 4.9, 7.3, 9.6, and 14 mM. The effect of an interferent species (ascorbic acid; AA) was also investigated. The optimized electrode structure for PPF/GOx/CNT/Co/Ti/Cr was that specified in Figure 3c. The polarization potential was +0.8 V vs Ag/AgCl with an electrolyte of pH 7.4 20 mM phosphate buffer solution. Inset: enlargement of the region for lower glucose concentrations of 0.25, 0.49, 0.73, 0.96, 1.4, and 1.9 mM.

We now consider the final step of PPF overcoating. The structure of the PPF is often different from that of the original monomer. The structure of acetonitrile PPF consists of highly branched and incompletely cross-linked aliphatic hydrocarbon backbone chains containing nitrogen atoms in the form of primary amine groups.[29] Immobilization of the PPF-overcoating of adsorbed GOx has four important aspects: (i) no cross-linking agent should be used that may damage the active sites of the enzymes; (ii) the acetonitrile PPF plays a role as the matrix of a biocompatible microenvironment for enzyme activity to enhance the enzyme electrode sensitivity, because the polymer backbone has a hydrophilic nature;[30] (iii) passivation for separation of each CNT island; and (iv) as an antifouling coating on the exposed Cr layer where CNTs are not grown.[31] It is noteworthy that GOx retains its enzymatic activity, despite being exposed to high-energy plasma. This means that the mild organic plasma employed is suitable for processes involving biomaterials. Therefore, the plasma-polymerized process is an effective strategy for the fabrication of an enzyme-friendly platform in CNT-based amperometric biosensors.

Sensor Performance. The previous sections have presented the optimization of the sensor fabrication process based on CNTs and the PPF. In this section, the performance of the optimized biosensor device is demonstrated. Amperometric measurements are widely used to evaluate and analyze the performance of glucose biosensors toward an increase in glucose concentration. Figure 4 shows the steady state amperometric response of the fabricated biosensor at +0.8 V vs Ag/AgCl. From the cyclicvoltanmetry in Figure 3, the potential at more than +0.6 V is available for time-base measurement with the fixed potential. The reason why +0.8 V is chosen is that the higher potential enables the high sensitivity. In spite of the high potential, the interfering substance (ascorbic acid) is negligible in the sensing characteristics (discuss below). A sequential increase in the glucose concentration at regular intervals is observed, of which the linear

range of glucose concentrations (0.25−19 mM) can cover the physiological range (discussed with Figure 5). The small background current (50−70 μA cm^{-2}) compared with the glucose response (240 μA cm^{-2} of 2.5 mM glucose) is a significant characteristic in the present results, because other CNT-based biosensor with directly grown CNT have exhibited higher background current.[20,22,23] This means that there is no need to calibrate the baseline for the glucose measurement. The detection limit was 34 μM when the signal-to-noise ratio was 3. The response time (95% to maximum response) was less than 7 s.

Figure 4 also shows a comparison of the amperometric response to an interference agent (ascorbic acid) and glucose. The maximum level of ascorbic acid under physiological conditions is 0.5 mM, which is larger than any other materials such as acetaminophen and uric acid. The current of 17 μA cm^{-1} in response to 0.5 mM ascorbic acid was similar to the response for 0.22 mM glucose; therefore, the interference is negligible for use in physiological samples. The albumin is also abundant in blood smale. It is a macromolecule protein and an electrochemically inactive material. This is easily eliminated with the use of membrane such as cellulose and Nafion. Of course, it can be adopted in our device. It will be the next step. The biosensor has

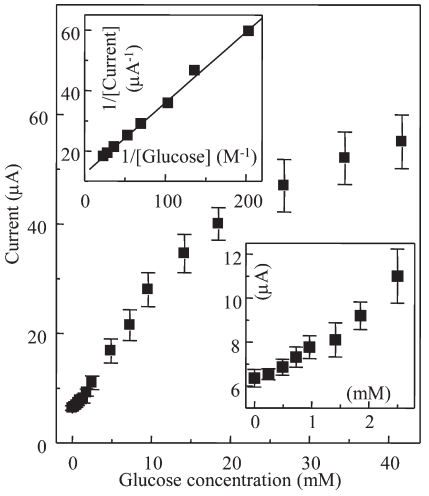

Figure 5. Calibration plot for glucose response using the data in Figure 4. Correlation line in glucose concentration range (0.25−19 mM); sensitivity of 38 μA mM^{-1} cm^{-2} (r = 0.993). Lower inset: enlargement of the low concentration range. Upper inset: Lineweaver−Burk plot. I_{max}, 0.32 mA cm^{-2}; K_M^{app}, 19 mM. Each point represents the average and the vertical bars designate the standard deviation (n = 4).

this characteristic because the PPF process provides a nano/micro scale environment for the GOx-PPF-CNT interface, thereby enhancing the electron transfer between the active sites of the enzymes and the electrode and reducing the antifouling effect (low background current and low response to interferents).

Figure 5 shows the current vs glucose concentration based on the data from Figure 4. The sensor response covers a wide range of glucose concentrations (0.25−19 mM) with good linearity (correction coefficient r = 0.994), and the sensitivity determined from the slope is 38 μA mM^{-1} cm^{-2}. Saturation from linearity is observed at higher (>20 mM) glucose concentrations, which represents a typical characteristic of the Michaelis−Menten model. The upper inset of Figure 5 shows a Lineweaver−Burk plot. The apparent Michaelis−Menten activity (K_M^{app}), as an indication of the enzyme−substrate kinetics for the biosensor, can be calculated from a double reciprocal plot

$$\frac{1}{I} = \frac{K_M^{app}}{I_{max}}\frac{1}{C} + \frac{1}{I_{max}} \quad (3)$$

where I is the steady-state current, I_{max} is the maximum current under stationary substrate conditions, K_M^{app} denotes the apparent Michaelis constant, and C is the glucose concentration. The I_{max} and K_M^{app} values were obtained from extrapolation of the plot shown in the upper inset of Figure 5. K_M^{app} was thus estimated to be 19 mM, which is similar to that for other CNT-based biosensors[28,31] and is smaller than that for GOx in solution (33 mM).[32] This shows that immobilized GOx has an increased affinity toward the substrate (glucose). The obtained maximum current density of 0.32 mA cm^{-2} is comparable to those of other CNT-based biosensors.[24,32,33]

Table 1 shows a comparison of the characteristics and performance of the fabricated biosensors are compared with those for other glucose biosensors that contain CNTs and other nanomaterials and were fabricated by various processes. It is confirmed that the present sensor exhibited similar or better performance compared with the other reported biosensors. It should be emphasized that the proposed dry chemical process for fabrication of a biosensor is simple, robust, reproducible, and reliable, i.e., there are no requirements for cumbersome modification steps, e.g., "wiring" of the enzyme[32] and self-assembled reconstruction of the apoenzyme.[33]

The operational stability was investigated under continuous polarization at +0.8 V in the presence of 19 mM glucose. The electrochemical response of the device retained a current response greater than 95% of the initial current after 24 h.

Table 1. Comparison of the Performance Parameters of Glucose Biosensors on Carbon Nanotubes and Other Nanomaterials

electrode	sensitivity (μA mM^{-1} cm^{-2})	linear range (mM)	detection limit (μM)	applied potential (V)	response time (s)	ref
PPF/GOx/CNT(direct growth)/Co/Ti/Cr	38	0.25−19	34	0.8	7	this work
GOx/CNT(direct growth)/Co/Ti/Cr	20.6	2−8	N/A	0.25	<5	19
GOx/Au−Pd/CNT(direct growth)/Pd/Ti	5.2	0.01−50	1.3	0.5	6	22
PPF/GOx/CNT(powder)/PPF/Au	42	0.025−2.2	100	0.8	<4	24
GOx/CS-CNT(powder)/PANI/Au[a]	21	1−20	10	0.5	5	17
GOx/CNT(powder)/PDDA/Au[b]	5.6	0.02−2.2	30	0.6	<20	15
GOx/CNT(powder)/POAP/Au[c]	11.4	0.02−10	50	0.75	<3	18
GOx/ZnO nanowire/Au	19.5	0.2−20	1	0.8	<5	10
GOx/ZnO nanofiber/Au	70.2	0.25−19	17	0.8	4	9

[a] Chitosan-coupled CNT/polyaniline. [b] Polydiallyldimethylammonium chloride. [c] 4-Poly(*o*-aminophenol).

The storage stability of the electrode was studied over the period of 7 days by storing it in buffer at 4 °C and recording the current (at +0.8 V in the presence of 19 mM glucose) at 1 days interval. The response tends to be practically constant and can still retain ca. 90% of its original response even after 7 days. These results suggest that the acetonitrile PPF overcoating layer prevents leaching and contamination of the GOx and CNTs components.

CONCLUSION

A novel method that provides for simple and reliable fabrication of a CNT-based amperometric biosensor using CNTs grown directly on a substrate that are covered with a PPF. This is continuous process for the designing CNT-based enzyme biosensors, because all processes are dry, except the enzyme immobilization procedure. The directly grown CNTs are treated with nitrogen plasma to change the surface from hydrophobic to hydrophilic in order to obtain an electrochemical contact between the CNTs and enzymes. The GOx enzyme was then adsorbed onto the CNT surface and the GOx layer was directly treated by acetonitrile plasma. In those, we stress again that the PPFs and/or plasma polymerization process plays a main role as such novel approaches to fabrication. The optimized glucose biosensor exhibited a wide dynamic range, rapid response, and selectivity toward the target species. This study may provide a simple and economic way to meet industrial requirements for the mass production of biosensors.

ASSOCIATED CONTENT

Supporting Information. Schematic illustration of the CNT growth apparatus. Optical photograph of the working electrode surface with CNTs and PPF (PDF). Detailed amperometric data with fixed potential. This material is available free of charge via the Internet at http://pubs.acs.org.

AUTHOR INFORMATION

Corresponding Author

*Tel.: +81-3-5859-8320. Fax: +81-3-5859-8201. E-mail: muguruma@shibaura-it.ac.jp.

REFERENCES

(1) Hu, Y.; Wilson, G. S. *J. Neurochem.* **1997**, *68*, 1745–1752.
(2) Ishikawa, M.; Schmidtke, D. W.; Raskin, P.; Quinn, C. A. P. *J. Diabetes Complications* **1998**, *12*, 295–301.
(3) Merkoçi, A.; Pumera, M.; Llopis, X.; Pérez, B.; Valle, M.; Alegret, S. *Trends Anal. Chem.* **2005**, *24*, 826–838.
(4) Wang, J.; Lin, Y. *Trends Anal. Chem.* **2008**, *27*, 619–626.
(5) Pumera, M.; Ambrosi, A.; Bonanni, A.; Chng, E. L. K.; Poh, H. L. *Trends Anal. Chem.* **2010**, *29*, 954–965.
(6) Guo, C. X.; Sheng, Z. M.; Shen, Y. Q.; Dong, Z. L.; Li, C. M. *ACS Appl. Mater. Interfaces* **2010**, *2*, 2481–2484.
(7) Cheng, T.-M.; Huang, T.-K.; Tung, S.-P.; Chen, Y.-L.; Lee, C.-Y.; Chiu, H.-T. *ACS Appl. Mater. Interfaces* **2010**, *2*, 2773–2780.
(8) Guo, S.; Dong, S. *Trends Anal. Chem.* **2009**, *28*, 96–109.
(9) Ahmad, M.; Pan, C.; Luo, Z.; Zhu, J. *J. Phys. Chem. C* **2010**, *114*, 9308–9313.
(10) Pradhan, D.; Niroui, F.; Leung, K. T. *ACS Appl. Mater. Interfaces* **2010**, *2*, 2409–2412.
(11) Yang, K.; She, G.-W.; Wang, H.; Ou, X.-M.; Zhang, X.-H.; Lee, C.-S.; Lee, S.-T. *J. Phys. Chem. C* **2009**, *113*, 20169–20172.
(12) Li, J.; Wang, Y.-B.; Qiu, J.-D.; Sun, D.-C.; Xia, X.-H. *Anal. Bioanal. Chem.* **2005**, *383*, 918–922.
(13) Kim, J.; Baek, J.; Kim, H.; Lee, K.; Lee, S. *Sens. Actuators, A* **2006**, *128*, 7–13.
(14) Rakhi, R. B.; Sethupathi, K.; Ramaprabhu, S. *J. Phys. Chem. B* **2009**, *113*, 3190–3194.
(15) Yan, X. B.; Chen, X. J.; Tay, B. K.; Khor, K. A. *Electrochem. Commun.* **2007**, *9*, 1269–1275.
(16) Wang, Z.-G.; Wang, Y.; Xu, H.; Li, G.; Xu, Z.-K. *J. Phys. Chem. C* **2009**, *113*, 2955–2960.
(17) Wan, D.; Shaojun, Y.; Li, G. L.; Neoh, K. G.; Kang, E. T. *ACS Appl. Mater. Interfaces* **2010**, *2*, 3083–3091.
(18) Pan, D.; Chen, J.; Yao, S.; Tao, W.; Nie, L. *Anal. Sci.* **2005**, *21*, 367–371.
(19) Cai, C.; Chen, J. *Anal. Biochem.* **2004**, *332*, 75–83.
(20) Chen, Y.-S.; Huang, J.-H.; Chuang, C.-C. *Carbon* **2009**, *47*, 3106–3112.
(21) Lin, Y.; Lu, F.; Ren, Z. *Nano Lett.* **2004**, *4*, 191–195.
(22) Wang, S. G.; Zhang, Q.; Wang, R.; Yoon, S. F. *Biochem. Biophys. Res. Commun.* **2003**, *311*, 572–576.
(23) Claussen, J. C.; Franklin, A. D.; Haque, A.; Porterfield, D. M.; Fisher, T. S. *ACS Nano* **2009**, *3*, 37–44.
(24) Muguruma., H. *Trends Anal. Chem.* **2007**, *26*, 433–443.
(25) Muguruma, H.; Shibayama, Y.; Matsui, Y. *Biosen. Bioelectron.* **2008**, *23*, 827–832.
(26) Muguruma, H.; Kase, Y.; Murata, N.; Matsumura, K. *J, Phys. Chem. B* **2006**, *110*, 26033–26039.
(27) Muguruma, H.; Kase, Y. *Biosens. Bioelectron.* **2006**, *22*, 737–743.
(28) Khare, B.; Wilhite, P.; Tran, B.; Teixeira, E.; Fresquez, K.; Mvondo, D. N.; Bauschlicher, C., Jr.; Meyyappam, M. *J. Phys. Chem. B* **2005**, *109*, 23466–23472.
(29) Hiratsuka, A.; Muguruma, H.; Nagata, R.; Nakamura, R.; Sato, K.; Uchiyama, S.; Karube, I. *J. Membr. Sci.* **2000**, *175*, 25–34.
(30) Muguruma, H.; Hiratsuka, A.; Karube, I. *Anal. Chem.* **2000**, *72*, 2671–2675.
(31) Tang, H.; Chen, J.; Yao, S.; Nie, L.; Deng, G.; Kuang, Y. *Anal. Biochem.* **2004**, *331*, 89–97.
(32) Gooding, J. J.; Wibowo, R.; Liu, J.; Yang, W.; Losic, D.; Orbons, S.; Mearns, F. J.; Shapter, J. G.; Hibbert, D. B. *J. Am. Chem. Soc.* **2003**, *125*, 9006–9007.
(33) Patolsky, F.; Weizmann, Y.; Willner, I. *Angew. Chem., Int. Ed.* **2004**, *43*, 2113–2117.